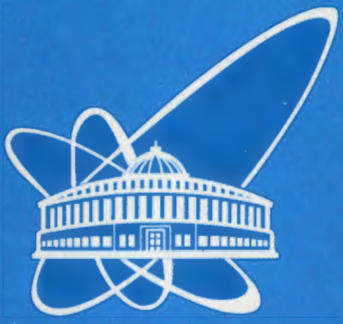

СООБЩЕНИЯ
ОБЪЕДИНЕННОГО
ИНСТИТУТА
ЯДЕРНЫХ
ИССЛЕДОВАНИЙ

Дубна

E9-2000-294

A.V.Elzhov, A.K.Kaminsky, V.I.Kazacha, E.A.Perelstein,
S.N.Sedykh, A.P.Sergeev

STUDY OF SCHEME OF TWO-BEAM ACCELERATOR DRIVER WITH ACCOMPANYING ELECTROMAGNETIC WAVE

2000

INTRODUCTION

Some schemes of the two-beam accelerator (TBA) driver based on a linear induction accelerator (LIA) were discussed in [1–4]. In these schemes the driver electron beam moves through a row of alternating microwave generators (free electron lasers (FEL), relativistic klystrons, etc.) and reaccelerating sections. The microwave power is totally extracted after every generation section. This kind of driver was experimentally investigated in [5], where reacceleration of a bunched electron beam travelling through two induction accelerator cells was demonstrated. The continuous extraction of the microwave power along the whole driver length was designed in CLIC [6] and the corresponding beam dynamics was also studied in [7].

A new scheme of TBA driver based on a linear induction accelerator was suggested in [8]. The scheme has the following characteristic properties:

a) the electron beam bunching occurs at a rather low ~ 1 MeV initial energy;
b) the bunched beam further acceleration occurs in the accompanying enhanced microwave that provides the steady longitudinal beam bunching along the whole driver;
c) there is no total microwave power extraction anywhere in the driver. Besides, partial extraction is needed to provide the quasi-stationary beam transition and RF field sufficient for maintaining the beam bunching;
d) a beam-loaded smooth waveguide is used along the driver.

The driver consists of an injector, buncher and long (a few hundred meters) row of separate LIA sections producing the external accelerating electric field and partitioned by transition chambers. The injector produces the initial electron beam with an energy of 1 through 2 MeV and a current of 0.5 through 1 kA. This beam is injected into the buncher. It may be a travelling wave tube (TWT) working in the amplification mode. It was shown in [9] that a high degree of bunching can be rather easily achieved in the TWT at the distance of ~ 1 m. Then the electron bunches continue moving in the LIA in accompaniment with the microwave enhanced in the TWT. The accelerating electric field may be applied continuously along the whole driver length or only in discrete accelerating gaps. The microwave power extraction from the driver occurs only in the transition chambers. The

system attains the steady state at first few tens of meters where the bunch energy increases up to the level of ~ 10 MeV. Then the section of quasi-stationary microwave generation begins where the total power, the accelerating field inserts into the beam, transforms into the microwave power.

The scheme has the following merits:

1) a possibility of providing the microwave phase and amplitude stability. The phase stability can be obtained at the expense of quasi-continuity of the system. It means that only mechanical tolerances will be significant.
2) due to the bunched beam acceleration it is not necessary to have the electron beam bunching at the energy of ~ 10 MeV.

1. SIMULATION OF ACCELERATION OF ELECTRON BUNCHES ACCOMPANIED BY ELECTROMAGNETIC WAVE IN EXTERNAL ELECTRIC FIELD

We have three characteristic regions of the driver:

1) bunching region with a TWT and without acceleration;
2) transition region with beam acceleration;
3) quasi-stationary beam propagation region.

As it was shown in [9], one can obtain the electron beam bunching in a TWT at a rather short length of ~ 50 cm for the electron beam and E_{01} type microwave parameters presented in Table 1.

Table 1. Beam and wave parameters for the TWT buncher used in the simulation [9].

Electron beam energy	~ 2.2 MeV ($\gamma_0 \sim 5.31$)
Electron current inside TWT I_b	~ 500 A
Electron beam radius	~ 0.5 cm
Microwave frequency f_0	17 GHz ($\lambda \sim 1.76$ cm)
Initial microwave power in TWT	10 kW
TWT output microwave power at the transition region entrance	13 MW

Without the accompanying microwave, the debunching process will immediately occur at the distance of about few tens of centimeters. The simulation has shown that the electron bunches can be transported at the distance of ~ 10 m if the microwave accompanies the bunches. The most encouraging situation is when the moving bunches are simultaneously accompanied by the amplified microwave and accelerated in the external electric field inside a corrugated waveguide. The waveguide must be transparent for the pulse accelerating field and a good screen for the microwave.

The following system of differential equations has been used for the simulation of the bunched beam acceleration after the TWT output [7,9,10]:

$$\frac{dW_j}{d\zeta} = -F\cos\psi_j + \varepsilon_0, \tag{1}$$

$$\frac{d\vartheta_j}{d\zeta} = 2\gamma_0^2(\Delta_0 + \frac{1}{\beta_{zj}} - \frac{1}{\beta_{z0}}), \tag{2}$$

$$\frac{dF}{d\zeta} = 2\pi J < \cos\psi_j > -\Gamma F \ , \tag{3}$$

$$F\frac{d\varphi}{d\zeta} = -2\pi J < \sin\psi_j > . \tag{4}$$

Here $W_j = \gamma_j/\gamma_0$ is the normalized energy of the j-th particle, $\zeta = k_0 z/2\gamma_0^2$ is the longitudinal dimensionless coordinate, $k_0 = \omega_0/c$ is the wave number in the free space, $\omega_0 = 2\pi f_0$ is the microwave frequency. The value θ_j is the phase of the j-th electron relative to the electromagnetic field; φ is the phase of the microwave complex amplitude ($\hat{F} = F\exp(i\varphi)$), $\psi_j = \varphi + \theta_j$ is the total ponderomotive phase. The value $F = 2\gamma_0 e|E_z|/mc\omega_0$ is the dimensionless amplitude of the microwave longitudinal electric field. Parameter $\Delta_0 = 1/\beta_{z0} - 1/\beta_{ph}$ defines the initial detuning of the wave-particle synchronism; β_{zj} is the longitudinal dimensionless electron velocity, and β_{ph} is the microwave phase velocity the waveguide should be designed for. The parameter $\varepsilon_0 = 2\gamma_0 eE_a/m\omega_0 c$ is dimensionless value of the external electric field E_a; the parameter Γ is the attenuation constant characterizing the distribution of the microwave losses along the driver.

The brackets in the equations (3) and (4) denote an average over the bucket. We define the bunching parameter as $B = |< e^{i\psi} >|$ [11].

The processes of the preliminary beam bunching and the microwave amplification in a TWT may be simulated by the same system of equations where the ε_0 and Γ values are equal to zero.

The beam-microwave interaction parameter J is proportional to the cubed Pierce parameter value:

$$J = \frac{2\gamma_0^3}{\pi m c^2/e} IZ, \tag{5}$$

where

$$Z = \frac{|E_z^2|}{2k_0^2 N} \tag{6}$$

is the beam-wave coupling impedance (N is the wave power in the given mode). The coupling impedance for beams in slowing structures is derived in Appendix A.

Now let us proceed to the beam-wave interaction immediately in the driver. We can evaluate the necessary steady state parameters from (1–4) to provide the quasi-stationary beam transition along the driver. Taking into account that the beam is bunched in the vicinity of $\psi \approx \pi/2$ we obtain

$$\psi \approx \pi/2 - \varepsilon_0/F, \quad \Gamma \approx 2\pi\varepsilon_0 J/F^2 \text{ and } \quad 2\gamma_0^2(1/\beta_{zj} - 1/\beta_{ph}) - 2\pi J/F^2 = 0. \tag{7}$$

The beam and wave simulation parameters correspond to the ones obtained at the TWT output under the conditions stated above (Table 1). The beam at the buncher input is monoenergetic with the beam longitudinal velocity $\beta_{z0} = \beta_0$ corresponding to the relativistic factor of γ_0. To estimate the values of Γ and β_{ph}, we took the amplitude F value from the TWT bunching process calculation [9] and $\beta_{zj} \approx 0.9989$. Then we have $\Gamma \approx 0.18$ and the phase velocity in the steady state $\beta^* \approx 1.03$. (Note that it does not make any contradiction with Cherenkov condition for radiating particles, whose velocity is always less than the speed of light. The matter makes the effective shift of the microwave phase velocity in a beam-loaded waveguide as well as on the stage of preliminary beam bunching. The "beam loading effect" is discussed more in detail in Appendix B.)

In the transition region the beam has to be accelerated from the energy of ~ 2 MeV up to the energy of 10 MeV. It corresponds to increasing the microwave phase velocity β_{ph} from $\beta_0 \approx 0.982$ up to $\beta^* \approx 1.03$. In the simulation the following spatial function of β_{ph} was accepted:

$$\beta_{ph}(z) = \beta_0 + (\beta^* - \beta_0)(1 - \exp(-Kz)) \qquad (8)$$

where the $K = 0.0178$ cm^{-1}. To provide the space changing of the phase velocity, we must vary the corrugation amplitude, spatial period and the mean waveguide radius under the condition that the beam-microwave interaction parameter J does not change.

2. SIMULATION RESULTS

To specialize parameters Γ and β^* with respect to the first rough estimation (7), the system (1–4) for the close parameters values is solved. Minimizing the deviation of the microwave power from its average level inside the quasi-stationary beam propagation region, we get the following final parameters values: $\Gamma \approx 0.112$ and $\beta^* \approx 1.02$. The first set of calculations has been accomplished for the case when the external electric field E_a and the attenuation constant Γ are continuously distributed along the driver. The particle phase-energy distributions obtained at the TWT output were taken as the input data to calculate the steady state of the driver.

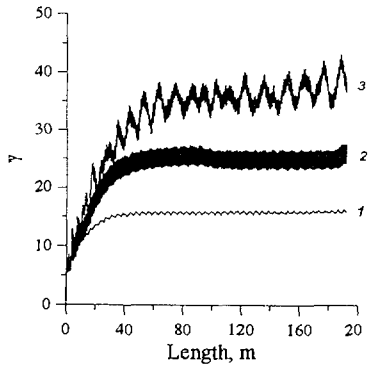

Fig. 1. The electron mean energy versus the distance for: 1 – continuously distributed driver parameters; 2 – discrete periodic cells, 3 – discrete cells with narrow accelerating gaps.

Our calculations have shown that the bunching process in the TWT must be interrupted a little bit earlier than the bunching parameter B attains its maximum value. Then we have no particle losses in our further calculations in the driver. Fig. 1 (curve 1) shows the calculated dependence of the bunch mean energy $\bar{\gamma}$ on the distance ($z = 0$ corresponds to the TWT output).

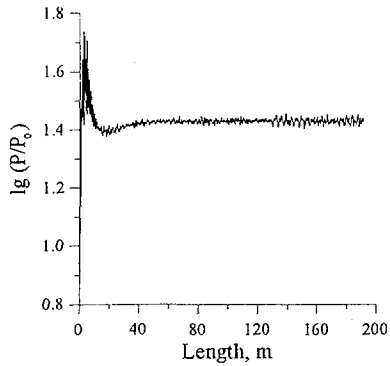

Fig. 2. The microwave power versus the distance for continuously distributed driver parameters. The power level P_0 at the driver input (TWT output) is about 13 MW.

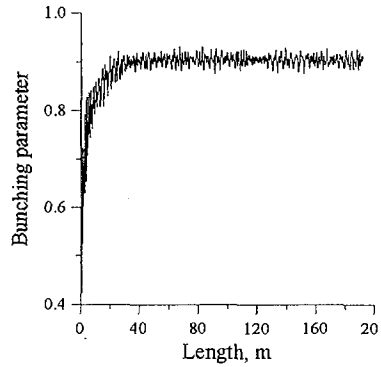

Fig. 3. The bunching parameter versus the distance for continuously distributed driver parameters.

The dependences of the microwave power and the bunching parameter B on the distance are presented in Figs. 2,3. As one can see from these figures, the steady state of the system is achieved at the distance of ~ 40 m. The power level of the transported microwave in the steady state is equal to ~ 330 MW. The mean steady state bunch energy is ~ 7.5 MeV. Besides, we have a rather high bunching parameter $B \sim 0.9$ in the steady state. The electron phase picture (Fig. 4) presents the distribution for a small beam fragment corresponding to the bunching period (the particle ensemble initially distributed uniformly in the phase interval $0 < \vartheta < 2\pi$). The appearance of "lagged" particles denotes the particle exchange between bunches.

The power per the length unity set into the electron beam by the external electric field is equal to ~ 500 MW/m. It transforms into the microwave power in the steady state.

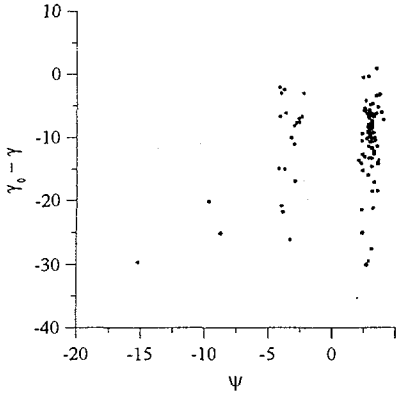

Fig. 4. The typical electron phase space picture at the distance of 100 m for continuously distributed driver parameters.

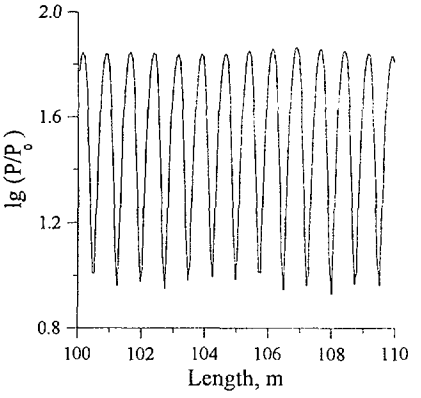

Fig. 5. The microwave power versus the distance from 100 m through 110 m for discrete periodic cells.

The stability of the steady state solution with respect to a possible error in the electron beam current I_b was also investigated. The calculations have shown that we still obtained the steady state solution up to the error values of $\delta I/I \approx \pm 10\%$.

A real LIA consists of separate induction sections partitioned by transition chambers, so that it has a discrete structure. The second set of our calculations was performed for the realistic induction section parameters. As a result, the optimal lengths of the induction sections (l_s = 50 cm) and transition chambers (l_t = 25 cm) were found. The microwave extraction was switched on only in the transition chambers. The electric field E_a was equal to 1.5 MV/m inside the accelerating sections. This corresponds to the same accelerating gradient averaged over the driver length as in the upper case of the uniform external electric field and microwave extraction.

The dependence of the bunch mean energy on the distance is shown in Fig. 1 (curve 2). One can see a short range of dependence of the microwave power along the distance of 10 m (from z = 100 m through z = 110 m) in Fig. 5.

In the third set of calculations for the same lengths of the accelerating sections and transition chambers the only difference was the following: accelerating voltage of every section (750 kV) was concentrated only on the gap 7.5 cm long located at the beginning of every section to make a more simple waveguide in this case. The dependence of the bunch mean energy on the distance is depicted in Fig. 1 (curve 3). The steady state also occurs when the system has the discrete structure. The bunching parameter B also stays high along the driver ($B \sim 0.9$). The microwave power amplitude stays rather stable.

3. FIRST SET OF EXPERIMENTS

The first set of our experiments was carried out with the the beam buncher. As the buncher we used a Cherenkov relativistic TWT made from thin copper previously used in [12]. It had the length of ~ 45 cm and main radius 9.1 mm.

We used the electron beam with the energy of ~ 600 keV, electron current ~ 150 A in the TWT and the beam radius ~ 5 mm in these experiments. The longitudinal uniform magnetic field with strength ~ 0.3 T was used for the beam focusing. The slowed-down electric-type wave E_{01} of the oversize cylindrical waveguide with the corrugated wall was chosen as an operating wave. The phase wave velocity $\beta_{ph} = 0.86$ at the operating magnetron frequency $f = 36.4$ GHz was close to the electron velocity. The scheme of these experiments is shown in Fig. 6.

The input signal at the wavelength $\lambda = 8.24$ mm was transmitted into the operating waveguide (8) from the magnetron (6) along the waveguide (5) with the help of the quasi-optical mirror (16). To prevent the parasitic self-excitation of the system, the smooth conjugation of the corrugated waveguide with the output horn was utilized. The quasi-optical mirror had a hole for the electron beam flight and was placed before the corrugated waveguide by using the device (17) so that the microwave power level at the TWT input was as high as possible. As a result, the microwave losses from the magnetron to the TWT input were ~ 13 dB, i.e. the initial power level in the TWT was ~ 5 kW.

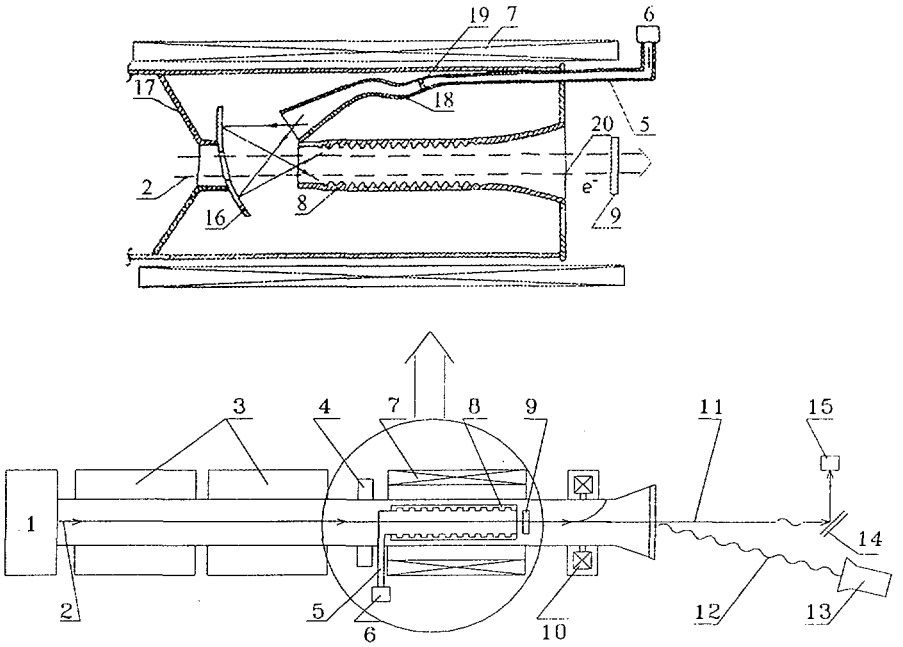

Fig. 6. Scheme of the experiment: 1) electron gun; 2) electron beam; 3) accelerating sections; 4) tuning magnetic lens; 5) microwave transmission line; 6) magnetron; 7) magnetic field coils; 8) decelerating corrugated cylindrical-surface waveguide; 9) quartz strip; 10) deflecting magnets; 11) optical Cherenkov radiation; 12) microwave radiation; 13) RF detector; 14) optical mirror; 15) streak camera IMACON-500; 16) quasi-optical mirror; 17) mirror fastening system; 18) mode transformer; 19) and 20) vacuum windows.

The microwave was transported from the magnetron onto the quasi-optical mirror through the special wave mode transformer (18) where the mode transformation took place according to the following scheme: $H_{10} \Rightarrow H_{11} \Rightarrow E_{01}$. The vacuum window in the output horn (20) was made of a polyamide film.

A numerical simulation of the beam bunching and microwave amplification was carried out. The electron density distribution in the beam cross-section is considered to have the "gaussian" form, i.e. it is $\propto \exp(-(r^2/r_{eff}^2))$ (see Appendix A). The distribution "tail" is certainly being cut by the waveguide ($r_{wg} = 9.1$ mm), so it needs to be normalized

properly. The rout-mean-square radius value, which is equal to r_{eff} exactly for "uncut" gaussian distribution, starts to deviate from it appreciably after $r_{eff} \approx 4.5 \div 5$ mm.

The calculated dependence of the microwave power on the distance from the buncher input for the mentioned above electron beam parameters is shown in Fig. 7. Fig. 8 shows the calculated spatial evolution of the bunching parameter B for our experimental conditions.

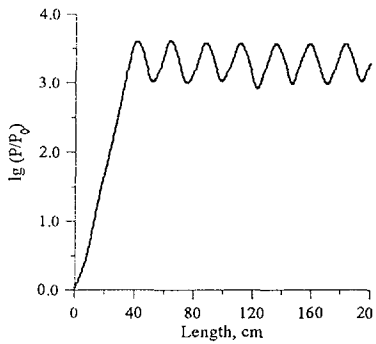

Fig. 7. The TWT microwave power versus the distance from the buncher output.

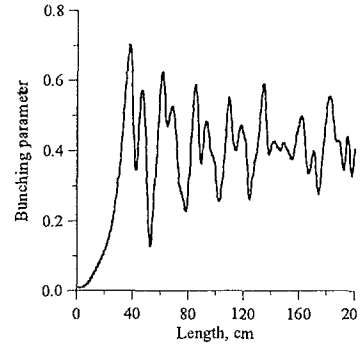

Fig. 8. The TWT bunching parameter versus the distance from the buncher output.

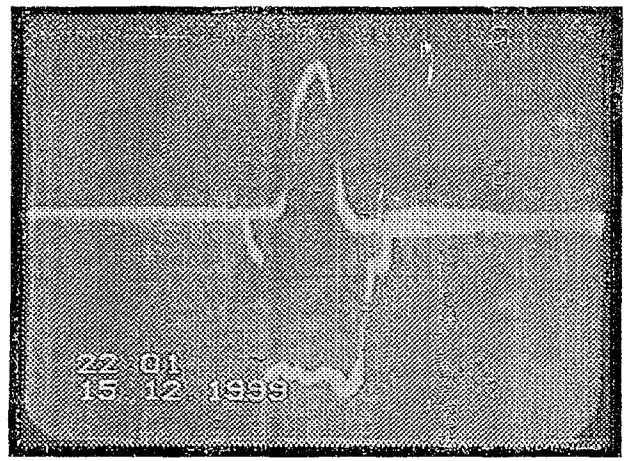

Fig. 9. The shape of the microwave power signal from the semi-conducting detector (upper trace) and electron beam current in the TWT (lower trace). The current amplitude is 150 A.

The calculated coupling impedance Z was ≈ 0.18 Ohms. The output microwave radiation consisted basically of the E_{01} wave and small admixture of asymmetrical waves. The microwave power and directional pattern were measured with the help of a calibrated semi-conducting detector. The corresponding signal from this detector is shown in Fig. 9 (upper trace). The microwave pulse duration was ~ 80 ns (at half maximum).

The measured maximum of the amplified microwave power was equal to ~ 5 MW with the gain ~ 30 dB. Coincidence with the calculations was rather good.

We used a quartz strip (3 mm thick, 3 mm wide and refractive index $n = 1.46$) for bunch dimension measurements. The target was placed on the electron bunch trajectory at the distance of ~ 80 mm from the TWT output (see Fig. 6). The electron bunches moved from the TWT exit to the quartz strip accompanied by the microwave, passed through the strip and generated Cherenkov radiation which was taken out through the vacuum window (20) (see Fig. 6). Hereupon Cherenkov radiation was directed to the input slit of the streak camera (15) by means of the optical mirror (14). The measured set of bunches is shown in Fig. 10. Sweep speed is equal to 13.3 ps/mm.

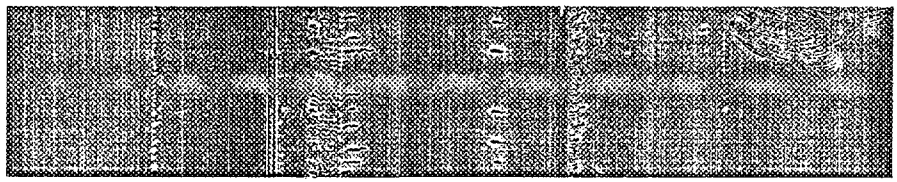

Fig. 10. Temporal profile of the bunched electron beam recorded by the streak camera.

The digitized set of these bunches is shown in Fig. 11 where the background was taken into consideration.

The corresponding Fourier spectrum is shown in Fig. 12.

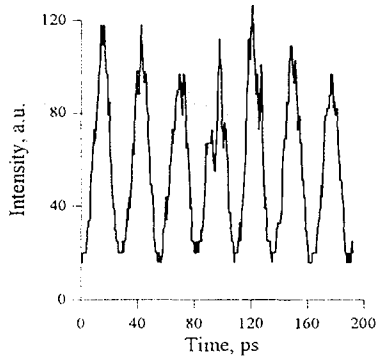

Fig. 11. Digitized intensity of Fig. 10 (in arbitrary units) plotted versus time.

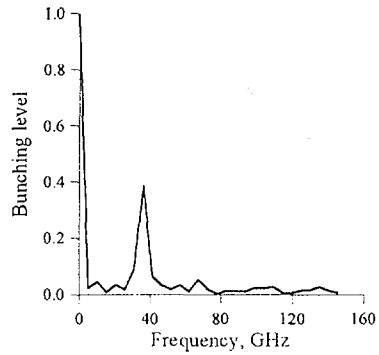

Fig. 12. Fourier spectrum of Fig. 11 (in terms of the bunching parameter).

We observe a significant peak at the frequency close to 36.4 GHz. The experimental bunching parameter is then defined as the ratio of the Fourier components at 36.4 GHz and zero frequency, respectively. The bunching parameter B was ~ 0.4 in our experiments that is close to the B value obtained in [13] at the beam energy of 2.2 MeV.

The numerical simulation has shown the electron bunches to be completely destroyed at ~ 4 cm after the TWT output if the beam is not accompanied by the amplified microwave. At the same time, the fulfilled experiments have confirmed that the electron bunches keep a high level of the bunching parameter at the distance of ~ 10 cm from the TWT exit being accompanied by the amplified microwave.

CONCLUSIONS

1. Our simulation has shown that a steady state could be found when electron bunches accompanied after a TWT by an amplified microwave are simultaneously accelerated in the external electric field both for continuously distributed system parameters and for discrete parameters of accelerating sections.

2. The total power, which is inserted into the beam by the accelerating field, transforms into the microwave power in the steady state. It was equal to ~ 500 MW/m in

our case. Such kind of systems can serve effectively as a rather long (hundreds of meters) driver for the TBA concept.

3. The first set of experiments, fulfilled with the buncher, has shown that the electron beam, accelerated in LIA-3000 and with a TWT allows us to obtain the necessary level of the amplified microwave power (~ 5 MW) and a high enough bunching parameter ($B \sim 0.4$) for carrying on further experiments with the TBA driver scheme. The electron beam bunching was registered with the help of Cherenkov radiation in the TWT amplifier at the frequency of 36.4 GHz.

4. The fulfilled experiments have also confirmed that the electron bunches keep a high level of the bunching parameter B at the distance of ~ 10 cm from the TWT exit being accompanied by the amplified microwave. The simulations made by means of the code PARMELA have shown that electron bunches debunch practically completely at this distance if they move without the microwave.

5. The planned test experiment based on the JINR LIA-3000 is expected to give a possibility of studying the bunching, microwave generation, beam propagation and twofold microwave extraction.

APPENDIX A. BEAM-WAVE COUPLING IMPEDANCE

For the slow wave of E_{01}-type in a waveguide with slightly corrugated walls, one can search for the solution of Maxwell's equations by means of Herz's vector [14] in the form: $\Pi = (0, 0, \Pi \exp(ik_z z))$, where $\Pi = \Pi_0 I_0(k_\perp r)$. ($I_0$ is the zero-order modified Bessel function). Here k_z is the longitudinal wave number, $k_\perp = \sqrt{k_z^2 - k_0^2}$ is the transversal wave number (k_0 – the wave number in the free space). (Note that calculating the k_z value one must take into account the additive due to the beam loading – see equation (B6) in Appendix B.) So the axial component of the electric field intensity is $E_z = -\Pi_0 k_\perp^2 I_0(k_\perp r)\exp(ik_z z)$.

The power of the given mode is $N = \mathrm{Re}\iint_{\sigma} S_z d\sigma = \frac{c}{4} k_z k_0 \Pi_0^2 \int_0^{k_\perp r_{wg}} I_1^2(\xi)\xi d\xi$, where S_z is the axial component of the complex Poynting's vector, σ is the waveguide cross-section ($d\sigma = r\, dr\, d\varphi$), r_{wg} is the mean waveguide radius.

For the beam having a pipe profile of radius r_b (6) yields:

$$Z = \frac{2k_\perp^4}{ck_z k_0^3} I_0^2(k_\perp r_b) \Big/ \int_0^{k_\perp r_{wg}} I_1^2(\xi)\xi d\xi . \qquad \text{(A1)}$$

For a paraxial electron beam let us suppose that the density has the Gaussian form, i.e. it is proportional to $\exp(-(r^2/r_{eff}^2))$. The distribution "tail" is certainly being cut by the waveguide, so it needs to be normalized properly. The rout-mean-square radius value, which is equal to r_{eff} exactly for the "uncut" Gaussian distribution, starts to deviate from it appreciably (decreasing) after $r_{eff} \sim r_{wg}/2$.

Considering the particle distribution as the superposition of rings of infinitesimal thickness and using the equation (A1), one can easily obtain the expression for the beam-wave coupling impedance. The function $I_0^2(k_\perp r)$ in (A1) will be replaced by its integral over the waveguide cross-section with the Gaussian weight, divided by a factor to account the cut-off of the Gaussian distribution within the radius r_{wg}:

$$Z = \frac{4k_\perp^4}{ck_z k_0^3 (1 - \exp(-(r_{wg}/r_{eff})^2))} \int_0^{r_{wg}/r_{eff}} \exp(-\xi^2) I_0^2(k_\perp r_{eff}\xi)\xi\, d\xi \Big/ \int_0^{k_\perp r_{wg}} I_1^2(\xi)\xi d\xi . \qquad \text{(A2)}$$

APPENDIX B. ELECTRON BEAM LOADING OF THE WAVEGUIDE

The distinctive feature of the TWT calculations is the large electron beam loading of the waveguide. It conduces to essential alteration of the microwave phase velocity and to the change of the wave-particle synchronism condition. To study the beam loading effects and, particularly, to determine the addition to the longitudinal wave number k_z, one can linearize the beam-wave equations [15] (the input beam is supposed to be monoenergetic).

Within the bunching region of the driver the equations (1–4) are valid at $\Gamma = \varepsilon_0 = 0$.

Let us take $\vartheta_j = \vartheta_{j0} + 2\gamma_0^2\Delta_0\zeta + \delta\vartheta_j$ and take into account that $\delta(\frac{1}{\beta_j}) = -\frac{1}{\beta_{z0}^3\gamma_0^2}\delta W_j$ for the longitudinal motion. Then, accepting

$$\delta W_j = \sum_m \delta\widetilde{W}_m \exp(i(\vartheta_{j0} + 2\gamma_0^2\Delta_0\zeta + \alpha_m\zeta)) + c.c. \qquad \text{(B1)}$$

$$\delta\vartheta_j = \sum_m \delta\widetilde{\vartheta}_m \exp(i(\vartheta_{j0} + 2\gamma_0^2\Delta_0\zeta + \alpha_m\zeta)) + c.c. \qquad \text{(B2)}$$

$$\hat{F} = \sum_m \delta\widetilde{F}_m \exp(i\alpha_m\zeta) \qquad (\hat{F} = F\exp(i\varphi)), \qquad \text{(B3)}$$

the system (1–4) reduces to a linear algebraic system for the complex amplitudes. The systems have non-trivial solutions under the following condition:

$$\alpha_m(\alpha_m + 2\gamma_0^2\Delta_0)^2 - 2\pi J/\beta_{z0}^3 = 0. \qquad \text{(B4)}$$

It determines the linear increment value for the microwave amplitude ($E_z \propto \exp(Gz)$)

$$G = -\frac{\omega_0}{2c\gamma_0^2}\operatorname{Im}\alpha_m, \qquad \text{(B5)}$$

and the additive to the longitudinal wave number due to the beam loading:

$$\delta k_z = -\frac{\omega_0}{2c\gamma_0^2}\operatorname{Re}\alpha_m. \qquad \text{(B6)}$$

This additive should be taken into account when the beam-wave coupling impedance is defined.

For the solutions having $\operatorname{Re}\alpha > 0$ the "loaded" wave phase velocity $\beta_{ph}^* = \omega/ck_z = \omega/c(k_{z0}+\delta k_z)$ is lower than the "unloaded" one. Particularly, the Cherenkov synchronism may be attained even when $\beta_{ph} > 1$.

To put it correctly, (B4) is not a simple cubic equation on α_m since factor J is a complicated function of k_z, and hence depends on α_m. However, within the framework of the linearized approach, one needn't solve (B4) exactly. The first iteration when the equation (B4) is solved for the non-perturbed J value turns out to be quite enough. The computing experience for the chosen waveguide geometry shows that the scale of the correction at the next iteration is lower by about one order of the magnitude.

In the case of exact initial synchronism (i.e. at $\Delta_0 = 0$) (B5) and (B6) are reduced to

$$G = \frac{\omega_0\sqrt{3}}{4c\gamma_0^2}\frac{\sqrt[3]{2\pi J}}{\beta_{z0}}, \quad \delta k_z = -\frac{\omega_0}{4c\gamma_0^2}\frac{\sqrt[3]{2\pi J}}{\beta_{z0}}. \tag{B7}$$

To illustrate the beam loading effect, we simulated the processes of beam-microwave interaction for a TWT oriented on various microwave velocities. For the electron beam the parameters of LIU-3000 facility (beam current of 200 A, electron energy 800 keV, beam cross-section radius $r_{eff} \sim 4$ mm) were taken. Fig. B1 presents the calculated from the system (1–4) dependence of the maximum microwave amplitude at the buncher output ($\propto F_{max}$) on the β_{ph} – the "unloaded" phase velocity of the wave.

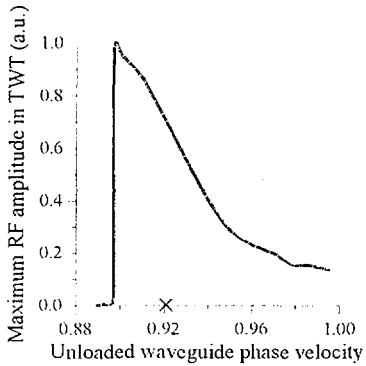

Fig. B1. Dependence of the microwave amplitude at the buncher output on the unloaded phase velocity β_{ph}. The cross corresponds to the initial electron beam velocity.

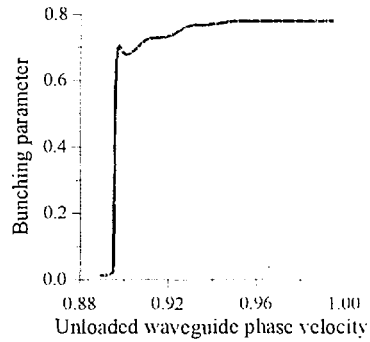

Fig. B2. Dependence of the bunching parameter on the unloaded waveguide phase velocity β_{ph}.

The cut-off character of the dependence is caused by the Cherenkov threshold. Availability of the amplifying effect when the longitudinal beam velocity $\beta_{\|} < \beta_{ph}$, is connected with the beam loading. The beam loading decreases the microwave phase velocity down to such a value β_{ph}^* when the wave-particle synchronism is established and the energy transfer from the electron beam to the microwave takes place. This effect allows us to use a smooth waveguide with $\beta_{ph} \approx 1$ in the LIA section. The similar kind of the dependence is given by the simulation for the electron beam bunching parameter B (also the maximum value at the end of the bunching process).

This work was supported by the Russian Fund for Basic Research, grants № № 97-02-16643, 98-02-17685.

REFERENCES

[1] A.M. Sessler, Proc. Workshop on the Laser Acceleration of Particles, eds. C. Yoshi and T. Katsouleas, AIP Conf. Proc. 91 (1982), p. 154.

[2] A.M. Sessler et al., Nucl. Instr. Meth., A306 (1991), p. 592.

[3] T. Houck et al., IEEE Trans. on Plasma Science, v. 24, 3 (1996), p. 938.

[4] G.G. Denisov et al., Nucl. Instr. Meth., A358 (1995), p. 528.

[5] T.L. Houck and G.A. Westenskow, Preprint UCRL-JC-119021, LNLL, Livermore, California, USA, 1994.

[6] W. Schnell, CERN-LEP-RF/86-27 (1986); CERN-LEP-RF/88-59 (1988).

[7] N.S. Ginzburg et al., in: Relativistic High-Frequency Electronics, v. 5 (IAP AS USSR, Gorky, 1988), p. 37 (in Russian).

[8] A.V. Elzhov, V.I. Kazacha, E.A. Perelstein, Proc. XV International Workshop on Linear Accelerators, ed. A.N. Dovbnya, v. II, Kharkov, 1997, p. 129.

[9] E.A. Perelstein, L.V. Bobyleva, A.V. Elzhov, V.I. Kazacha, JINR Preprint E9-97-5, Dubna, 1997.

[10] N.F. Kovalev, M.I. Petelin, M.D. Raiser, A.V. Smorgonsky, in: Relativistic High-Frequency Electronics (IAP AS USSR, Gorky, 1979), p. 76 (in Russian).

[11] H.D. Shay, R.A. Ryne, S.S. Yu and E.T. Scharlemann, Nucl. Instrum. Meth., 1991, A304, p. 262.

[12] O.V. Arkhipov et al., Proceedings of II EPAC, Nice (France), 1990, p. 34; JINR Preprint E9-91-50, Dubna, 1991.

[13] J. Gardelle et al., Proceedings of VI EPAC, Stockholm (Sweden), 1998, p. 463.

[14] L.A. Weinstein, Electromagnetic waves, Sovetskoe radio, Moscow, 1957 (in Russian).

[15] J.S. Wurtele, G. Bekefi, R. Chu and K. Xu, Phys.Fluids, B2 (2) (1990), p. 401.

Received by Publishing Department
on December 4, 2000.